Vol. 90 No. 2 pp. 525–536 ACTA GEOLOGICA SINICA (English Edition) Apr. 2016

Late-Quaternary Slip Rate and Seismic Activity of the Xianshuihe Fault Zone in Southwest China

ZHANG Yongshuang[1, 2, *], YAO Xin[1, 2], YU Kai[1, 2], DU Guoliang[1, 2] and GUO Changbao[1, 2]

1 *Institute of Geomechanics, Chinese Academy of Geological Sciences, Beijing 100081, China*
2 *Key Laboratory of Neotectonic Movement and Geohazard, MLR, Beijing 100081, China*

Abstract: The Xianshuihe fault zone is a seismo-genetic fault zone of left-lateral slip in Southwest China. Since 1725, a total of 59 $M_s \geq 5.0$ earthquakes have occurred along this fault zone, including 18 M_s 6.0–6.9 and eight $M_s \geq 7.0$ earthquakes. The seismic risk of the Xianshuihe fault zone is a large and realistic threat to the western Sichuan economic corridor. Based on previous studies, we carried out field geological survey and remote sensing interpretation in the fault zone. In addition, geophysical surveys, trenching and age-dating were conducted in the key parts to better understand the geometry, spatial distribution and activity of the fault zone. We infer to divide the fault zone into two parts: the northwest part and the southeast part, with total eight segments. Their Late Quaternary slip rates vary in a range of 11.5 mm/a – (3±1) mm/a. The seismic activities of the Xianshuihe fault zone are frequent and strong, periodical, and reoccurred. Combining the spatial and temporal distribution of the historical earthquakes, the seismic hazard of the Xianshuihe fault zone has been predicted by using the relationship between magnitude and frequency of earthquakes caused by different fault segments. The prediction results show that the segment between Daofu and Qianning has a possibility of $M_s \geq 7.0$ earthquakes, while the segment between Shimian and Luding is likely to have earthquakes of about M_s 7.0. It is suggested to establish a GPS or InSAR-based real-time monitoring network of surface displacement to cover the Xianshuihe fault zone, and an early warning system of earthquakes and post seismic geohazards to cover the major residential areas.

Key words: Xianshuihe fault zone, earthquake, left-lateral strike-slip fault, slip rate, seismic activity, prediction

1 Introduction

The Xianshuihe fault zone is an active left-lateral strike slip fault zone in Southwest China. As an important tectonic boundary, it has experienced a complicated tectonic evolution from the Paleozoic to Quaternary (Roger et al, 1995; Meade, 2007). It extends from Donggu of Ganzi County in the northwest through Luhuo County, Daofu County and Kangding County to Anshunchang of Shimian County in the south, about 350 km long and overall striking 320°–330°, appearing as an arc of slight protruding northeast (Qian et al., 1988; Zhang et al., 2004; Xiong et al., 2010). This fault zone is also an important intraplate seismic zone, along which many large earthquakes have occurred.

There have been many documents about the characteristics of the Xianshuihe fault zone (Heim, 1934; Tang et al., 1976, 1984; Schwartz and Coppersmith, 1984; Qian et al., 1988, 1990; Wen, 1988; Wen et al., 1989; Deng, 1989; Allen et al., 1991; Sun et al., 1994; Li et al., 1997; Tapponnier et al., 2001; Zhang et al., 2003; Wang et al., 2009; Li et al., 2015; Tang et al., 2015; He et al., 2015). Recent studies have focused on its Late Quaternary activities (Xu and Kamp, 2000; Lu and Liao, 2001; Cheng and Yang, 2002; Qiao et al., 2004; Tang et al., 2005; Ran and He, 2006; Peng et al., 2007; Wang et al., 2008; Yang and Su, 2007; Molnar and Dayem, 2010; Zhang et al., 2010, 2012, 2013; Wang et al., 2014; Li et al., 2015; Yan and Lin, 2015). Previous research has estimated or calculated the slip rate of the Xianshuihe fault zone by using different methods and marks. Allen et al. (1991) calculated the Holocene slip rate of the whole Xianshuihe fault zone as about 15 mm/a. He et al. (2006) suggested that the Late Quaternary strike-slip rate was approximately uniform along the entire length of the fault zone, about

* Corresponding author. E-mail: zhys100@sohu.com

15±2 mm/a. Tang and Han (1993) estimated the Holocene slip rate of the Xianshuihe fault zone to be (9±1)–(15±5) mm/a. Sun et al. (1994) obtained the left-lateral slip rate of about 10.9 mm/a for the Xianshuihe fault zone, but they did not give its time range. Xu et al. (1992, 2007) considered that the long-term average slip rate of the Xianshuihe fault zone since the Late Miocene was 8.4±1.7 mm/a. In addition, the slip rates of some member faults were also calculated (Deng, 1989; Wen et al., 1989; Qian et al., 1990; Li et al., 1997; Zhou et al., 2001; Chen et al., 2008). Considering remarkable left-lateral slip characteristic and frequent seismic activities of the Xianshuihe fault zone, our further field work and analysis suggest that its Late Quaternary slip rate is significant and that its seismic risk is a large and realistic threat to the western Sichuan economic corridor.

2 Geological Setting

The ground trace of the Xianshuihe fault zone can be clearly seen in remote sensing images, which is composed of several faults and shows certain segment ability (Fig. 1). According to the fault activity, Qian et al. (1988) divided it into five segments: the Donggu-Huiyuansi fault, Kangding fault, Yalahe fault, Zheduotang fault and Moxi fault. Furthermore, Li et al. (1997) divided the Donggu-Huiyuansi fault (also called northwest part) into three segments including the Luhuo fault, Daofu fault and Qianning fault in terms of geological and seismic investigation and large-scale regional active-faults mapping.

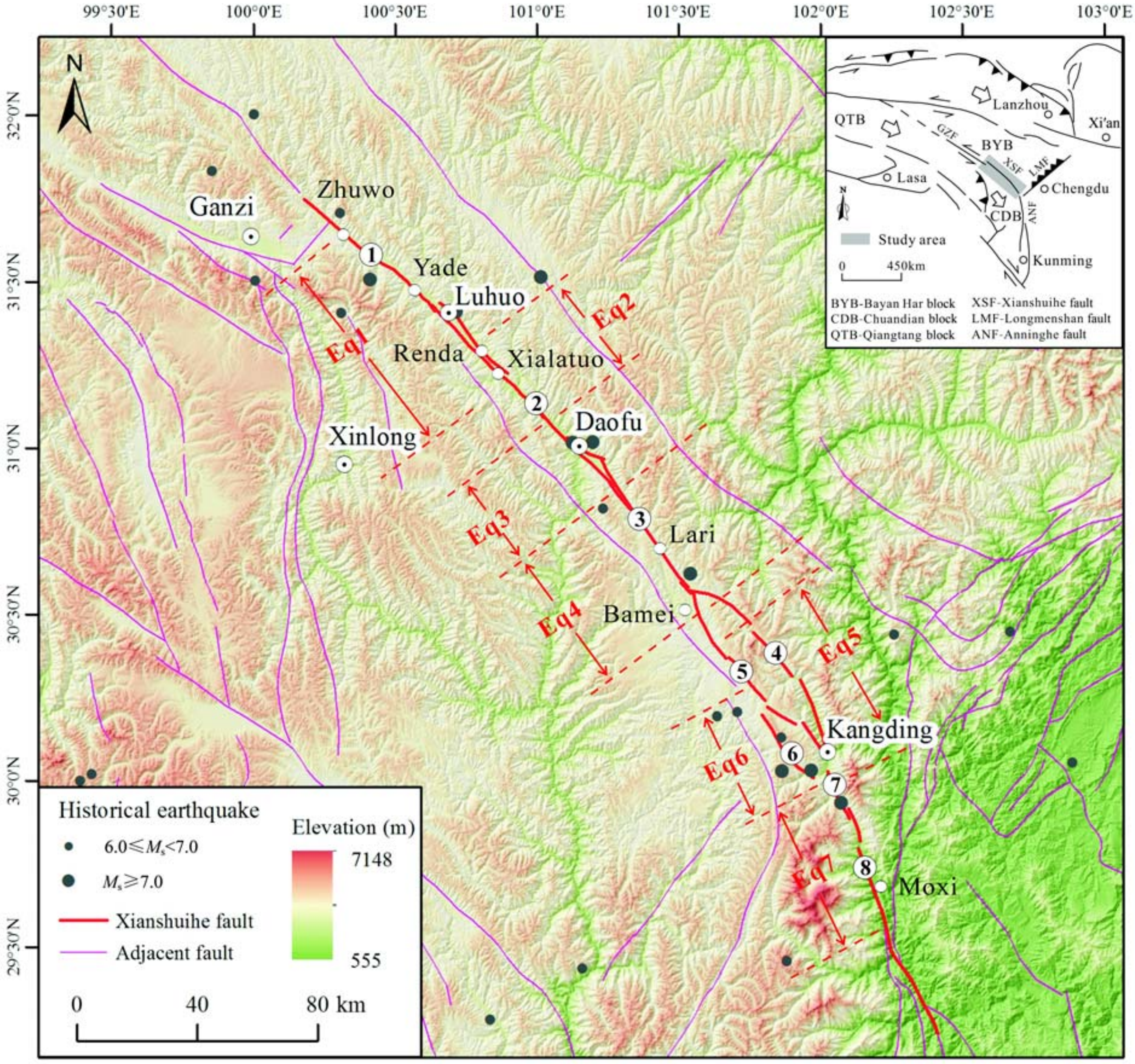

Fig. 1. Spatial distribution of the Xianshuihe fault zone and its related earthquakes since 1725.

Red arrows and dashed lines indicate the spatial extension of earthquake-induced surface ruptures. The numbers enclosed by circle indicate the various faults: ①, Luhuo fault; ②, Daofu fault; ③, Qianning fault; ④, Yalahe fault; ⑤, Zhonggu fault; ⑥, Zheduotang fault; ⑦, Kangding fault; ⑧, Moxi fault. Eq1, Luhuo earthquake in 1816 and 1973; Eq2, 1723 Changcu earthquake; Eq3, Daofu earthquake in 1904 and 1981; Eq4, 1893 Qianning earthquake; Eq5, 1725 Kangding earthquake; Eq6, 1955 Zheduotang earthquake; Eq7, 1786 Moxi earthquake.

Combining the former references and our investigation and research in recent years, we infer to divide the Xianshuihe fault zone into two main parts: the northwest part and the southeast part, with total eight segments (Fig. 1; Table 1). The northwest part is composed of the Luhuo fault with a length of 90 km, the Daofu fault with a length of about 85 km, and the Qianning fault with a length of about 62 km. They appear as left-order echelon and in landform are represented as a series of pull-apart basins such as the Xialatuo Basin, the Daofu Basin, and the Qianning Basin. The southeast part is composed of the Yalahe fault with a length of about 31 km, the Zhonggu fault with a length of about 21 km, the Zheduotang fault with a length of about 30 km, the Kangding fault with a length of about 80 km, and the Moxi fault with a length of about 40 km. Compared with those in the northwest segments, they are more complicated in form and structure.

3 Methods for Slip Rates Determination

On the basis of former studies, we carried out field geological survey and remote sensing interpretation in the Xianshuihe fault zone. Furthermore, geophysical exploration, trenching and age-dating were conducted in the key parts to better understand the geometry, spatial distribution, activity and seismic ruptures of the Xianshuihe fault zone.

The displacements of both sediment and geomorphic face are frequently used as marks for discrimination of activity time and rates of active faults. The sediment age may be the same as that of the geomorphic face, which can be directly used to estimate the fault slip rate. However, the sediment age may also be younger or older than that of the geomorphic face, which can be used to estimate the upper limit or lower limit of fault slip rate, respectively. Thus, the investigations of these symbols are important to obtain the reasonable slip rates of active faults. Among the following slip rates of the individual member faults in the Xianshuihe fault zone, some are our independent calculation, some from previous results, and some are our re-calculations based on new dating data. For the calculation of slip rate, precious dating is very important, but this is still a problem that is not fully resolved up to now.

4 Slip Rates of Member Faults in the Xianshuihe Fault Zone

4.1 Luhuo fault

The Luhuo fault mainly runs along low mountains and high terraces on the right bank of the Xianshuihe River. It dips either NE or SE with dip angles from 60° to 70° (Fig. 2). It seems to be of multiple activities: early dominated by thrust plus strike slip, and since Pleistocene by strike slip (Li et al., 1997). Horizontal offset landforms are often seen where it passed. It is most obvious that it made local river systems and gullies horizontally separated (Fig. 2).

From the remote-sense interpretation of ETM images and Spot images and combining with field investigation, we obtained the maximum horizontal offset of 2,100 m for Saqika gully northwest of the Luhuo County seat and the maximum horizontal offset of 1,800 m for Douri gully southeast of the Luhuo County seat. As far as we know, they are the maximum offsets occurred after Mid-Late Pleistocene in the Xianshuihe fault zone. On the other hand, corresponding to the above horizontal offsets, we obtained the thermoluminescence (TL) dating ages for the sand gravels, separated on the south side of Saqika gully: 191.65±21.08 ka and 172.20±18.94 ka. Thus, we calculated the slip rate since the Late Pleistocene to be (10.58±1.16) mm/a–(11.09±1.22) mm/a. Other horizontal offset data and dating data are listed in Table 2. On the whole, the average slip rate of the Luhuo fault since Late Pleistocene is 10–11.5 mm/a.

4.2 Daofu fault

The offset landforms formed by the left-lateral strike-slip of the Daofu fault are similar to those by the Luhuo

Table 1 Surface ruptures caused by earthquakes along the Xianshuihe fault zone since 1725 (modified from Wen et al., 1988; Li et al., 1997)

Seismo- generating fault name	Occurrence time	Epicenter site	Magnitude/M_s	Epicenter		Rupture scale (km)	Active feature
				Longitude (°)	Latitude (°)		
Kangding fault	1725.08.01	Kangding	7	101.83	20.16	50	Left-lateral
Moxi fault	1786.06.01	Moxi	$7^3/_4$	102.04	29.87	90	Left-lateral
Luhuo fault	1816.12.08	Luhuo	$7^1/_2$	100.75	31.29	>60	Left-lateral
Qianning fault	1893.08.29	Qianning	$7^1/_4$	101.37	30.70	70	Left-lateral
Daofu fault	1904.08.30	Daofu	7	101.00	31.06	55	Left-lateral
Daofu fault	1923.03.24	Changcu	7.3	100.90	31.17	60	Left-lateral
Zheduotang fault	1955.04.14	Zheduotang	$7^1/_2$	101.84	30.03	35	Left-lateral
Luhuo fault	1973.02.06	Luhuo	7.6	100.52	31.50	90	Left-lateral
Daofu fault	1981.01.24	Daofu	6.9	101.15	30.95	45	Left-lateral

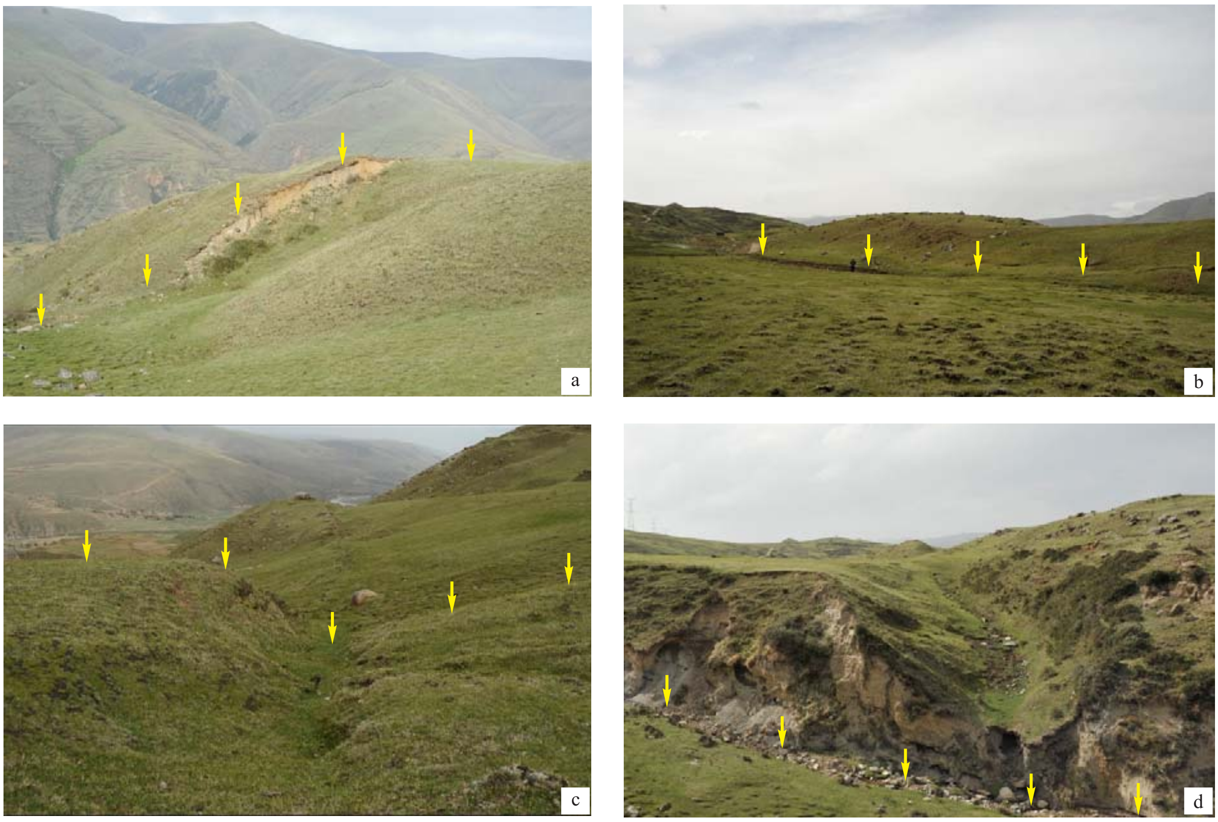

Fig. 2. Surface ruptures along the Luhuo fault during the 1973 Luhuo M_s 7.9 earthquake.
(a), Faulted ridge with left–lateral offset (NEE); (b), Fault scarps in the front of ridges (S); (c), Surface ruptures and fault troughs (NE); (d), Troughs along the fault (S).

Table 2 Horizontal offset data and dating data used to estimate the average slip rate of the Luhuo fault

No.	Position	Offset landform	Left-lateral offset (m)	Age of sediments（B.P.）	Horizontal slip rate（mm/a）	Data source
1	Kaqi gully	Drainages	2100	191.65±21.08 ka	10.58±1.16	This study
2	Douri gully	Drainages	1800	172.20±18.94 ka	11.09±1.22	This study
3	Northeast Kasu village	Drainages	212; 226; 210	21300±1150 a	9.98±0.54; 10.64±0.57; 9.89±0.53	This study
4	Yade Town seat	Gullies	148	21300±1150 a	7.0	Li et al., 1997
5	Dinggu village	Gullies	50.8	2830±160 a	18.0	Li et al., 1997
6	Zhanggu village	Gullies	38	3560 a，4190 a	11.0，9.0	Li et al., 1997
7	Laohekou	Drainages	46	3560 a，4190 a	13.0，11.0	Li et al., 1997

fault. Near Kewu village in Daofu County, for example, there are three gullies, of which two are blind gullies and one is a relative younger gully. Their arrangement was due to the horizontal offset along the Daofu fault. The horizontal offset between the two blind gullies is 82 m, and the horizontal offset between the younger gully and the blind gully (called gully 2) is close to 116 m. The total horizontal offset, i.e., the horizontal offset between the younger gully and the blind gully (called gully 1) far from it, is 198 m. According to Li et al. (1997), the age of gully 1 is 18975±360 a, and thus the average slip rate is 10.4 mm. But from the same landform evidence, Xu et al. (2003) gave a horizontal slip rate of 12±2 mm/a. Here we tentatively take 10–11 mm/a as the left-lateral strike-slip rate of the Daofu fault.

4.3 Qianning fault

The Qianning fault is almost covered by pluvial alluvial sediments, slope deposit and glacial till since Pleistocene (Fig. 3), but separated streams, gullies, small ridges, alluvial fans, and terraces. It is dominated by left-lateral strike-slip, but its hanging walls show some vertical drop. Its activities since Pleistocene have followed old fault planes, which have 60° to 80° dip angles, and of which, most dip SW and some dip NE.

Near Songlinkou, the Qianning fault made the T_2 terrace of the Zamaerke River 243 m horizontally left-lateral offset. According to Li et al. (1997), the age of the T_2 terrace is 21620±1500 a and the obtained average slip rate is 10.5–12.0 mm/a (Table 3). We measured the horizontal offset and age of the T_2 terrace in Songlinkou as 180 m

Fig. 3. Faulted scarps and pond along the Qianning fault.
(a), Rupture scarps on the southwest hillside of the Qianning basin (N); (b), Fault pond south of the Lari town seat (W).

Table 3 Horizontal offset data and dating data used to estimate the average slip rate of the Qianning fault

No.	Position	Offset landform	Left-lateral offset (m)	Age of sediments (B.P.)	Horizontal slip rate (mm/a)	Data source
1	Zamaerke River	T2 terrace	243	21620±1500a	10.5–12.0	Li et al.,1997
2	Songlinkou	Wetland margin	70	5933±99 a	11.8	Li et al.,1997
3	Taziba	T4 terrace	500–600	60 ka	8–10	Li et al.,1997
4	Songlinkou	T2 terrace	180	21620±1500a	8.37±0.38	This study
5	Longdengba	T2 terrace		18280±1000a		This study

and 21620±1500 a, respectively, and obtained a slip rate of 8.37±0.38 (Table 3). Here we would like to take 8–11 mm/a as the average slip rate of the Qianning fault over the past 20,000 years.

4.4 Zhonggu fault

The offset landforms of the Zhonggu fault are concentrated on its southeast end, mainly represented as the small offset of streams and gullies (Fig. 4). At a place 500 m northwest of Zhalagongma, we obtained a horizontal offset of 46.5 m. For no available dating data, we cannot obtain the slip rate there. Li (1997) estimated that the average slip rate of the Zhonggu fault was 3±1 mm/a.

4.5 Yalahe fault

The Yalahe fault shows a clear linear feature in remote sensing images. It is mostly covered by diluvium and talus and locally represented as troughs and scarps. Most scarps are 1–4 m high, and a few are up to 12 m high. Along the fault there occur dense hot springs, but there are not obvious landform marks which can be used to determine the horizontal offset. Considering that the Yalahe fault is similar in scale and activity time, intensity and characteristics similar to the Zhonggu fault (Fig. 4), we would like to take 3±1 mm/a as its average slip rate.

4.6 Zheduotang fault

New activities of the Zheduotang fault are embodied by

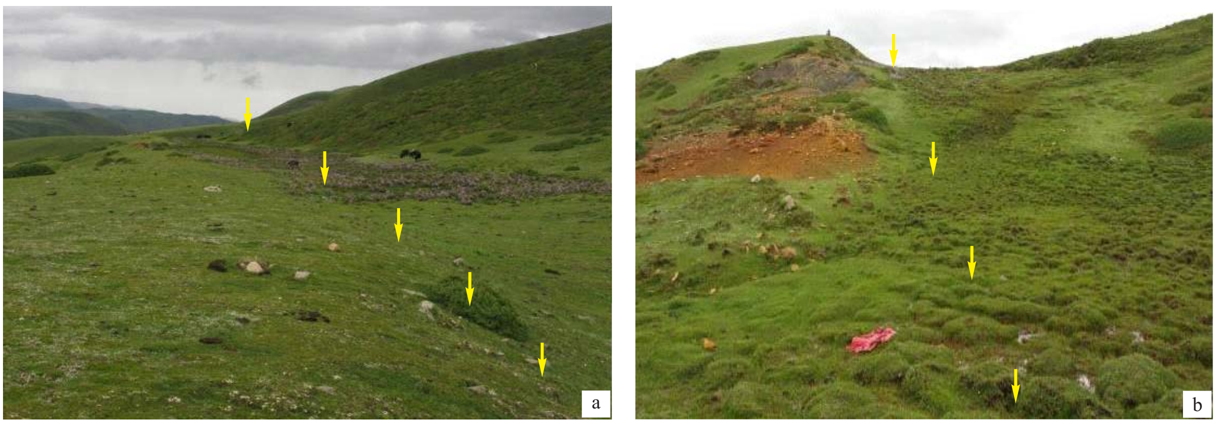

Fig. 4. Surface features of the Zhonggu fault.
(a), Intra-slope trough south to Jinlong Temple (315°); (b), Nek and intra-slope trough southeast to Jinlong Temple (320°).

offset of small ridges, alluvial fans, glacial till and talus (Fig. 5). North to Sidingcuo, a moraine dam shows a left-lateral slip of 15.50 m. The ^{14}C age of diluvium in the moraine dam is 6362 a BP, and so we obtained an average slip rate of 4.3 mm/a. And near Zheduo nek, the fault made a small gully 25.50 m left-lateral offset. The ^{14}C age of silty clay in the hanging wall of the fault is 4033±132 a BP, and so we obtained an average slip rate of 6 mm/a. On the whole, we would like to take 5±1 mm/a as the average slip rate of the Zheduotang fault since Holocene.

4.7 Kangding fault

The Kangding fault shows very remarkable offset landforms. It made streams, gullies, small ridges, and slope ridges horizontally offset (Fig. 6). For this fault, Li et al. (1997) gave four estimates of slip rate as shown in Table 4.

We observed that a gully near Laoyulin had a left-lateral offset of 185 m, and that a gully near Xinyulin had a left-lateral offset of 123 m. The TL age of the samples which we collected at the corresponding position is 26.63±2.26 ka. On the basis of this age, we estimated a left-lateral slip rate of 7.00±0.59 mm/a for the former and a left-lateral slip rate of 4.65±0.39 mm/a for the latter (Table 4). Combining with the slip rates by Li et al. (1997) in Table 4, it should be reasonable that 7–9 mm/a is taken as the average slip rate of the Kangding fault over the past 20,000 years.

4.8 Moxi fault

The Moxi fault is a member at the southernmost end of

Fig. 5. Surface features of the Zheduotang fault.
(a), Intra-slope troughs in Zheduoshan nek (SE); (b), Fault scarps near Kangding airport (NE).

Fig. 6. Surface traces along the Kangding fault.
(a), Fault scarps on the north slope of a road in Honghaizi; (b), Fault drumlin and fault pond northwest of Honghaizi.

Table 4 Horizontal offset data and dating data used to estimate the average slip rate of the Kangding fault

No.	Position	Offset landform	Left-lateral offset (m)	Age of the sediments	Horizontal slip rate (mm/a)	Data source
1	Cigalongba Gully	Moraine platform walls	150, 145, 160	22597±82a; 19800±1400a	6.6 7.7	Li et al.,1997
2	Selaha mountain nek	Gullies	34	2834±104a	12.0	Li et al.,1997
3	Mugecuo lake	Mid-ridge of moraine fan	116	18220±1400a	6.4	Li et al., 1997
4	Chongcaoping,YalaTown	Lateral moraine dam	7.5	786±101a	9.5	Li et al.,1997
5	Laoyulin	Gullies and drainages	185	26.63±2.26ka	7.00±0.59	This study
6	Xinyulin	Gullies and drainages	123	26.63±2.26ka	4.65±0.39	This study

the Xianshuihe fault zone. Its late activities are mainly represented as offset of terraces and alluvial fans and the bunchy distribution of hot springs (Fig. 7). We observed near Hailuo gully of Moxi Town, Kangding County that a sedimentary bed, corresponding with the micro-topography, shows a left-lateral offset of 800 m. The TL dating samples which we collected at the corresponding position yielded two ages: 93.05±7.91 ka and 97.23±8.26 ka. On the basis of these two ages, we estimated that the left-lateral slip rate of the Moxi fault during Holocene is 8.47±0.92 mm/a, which was consistent with both results of Zhang et al. (2007) and the long-term average slip rate.

Summing up the above, as far as the slip rate obtained by the geologic method is concerned, the northwest part of the Xianshuihe fault zone is higher in average slip rate than its southeast part. The average slip rates of the northwest part vary in the range of 8–12 mm/a, while that of the southeast part vary in the range of 3–9 mm/a. The northwest part is significantly higher than southeast. We think that the slip rate of Luhuo fault and Daofu fault has been roughly equivalent since Late Pleistocene, and that the average slip rate of Luhuo fault was 10–11.5 mm/a; the average slip rate of Daofu fault was 10–11mm/a; the average slip rate of Qianning fault was 8–11 mm/a, the slip rate of Zhonggu fault and Yalahe fault were low and both of them were 3±1 mm/a; the strike slip rate of Zheduotang fault has been 5±1 mm/a since the Holocene; the strike slip rate of Kangding fault was 7–9 mm/a; and the strike slip rate of Moxi fault was 8.47±0.92 mm/a. The low slip rates of Yalahe fault and Zhonggu fault, as well as Zheduotang fault, are mainly because they are located at the strike transition part of the fault zone (Fig. 1). The total slip rate of parallel-arranged faults, such as Yalahe fault and Zhonggu fault, approximates to the slip rate of their adjacent fault. The above results are by large comparable with the modern activity rates obtained by using short level observation data and GPS data (Wang et al., 2001; Cheng and Yang, 2002; Qiao et al., 2004 ; Tang et al., 2005 ; Peng et al., 2007).

5 Discussions

5.1 Characteristics of the seismic activities

Comprehensive analyses and our research show that the seismic activities along the Xianshuihe fault zone have the following three characteristics:

(1) The seismic activities along the Xianshuihe fault zone are frequent and strong. According to the historical records, since 1725, 59 $M_s \geq 5.0$ earthquakes have occurred along it, including 18 M_s 6.0–6.9 and eight $M_s \geq 7.0$ earthquakes (Fig. 8). The largest one was the Moxi M_s

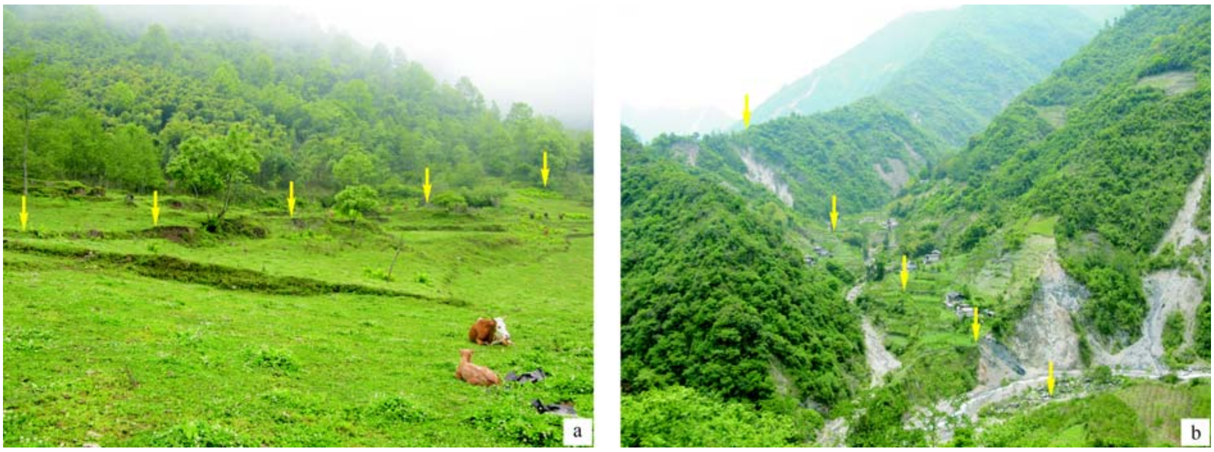

Fig. 7. Surface features of the Moxi fault.
(a), Fault scarp at Ertaizi (120°); (b), Offset of T_2 terrace at Shiyuewan (240°).

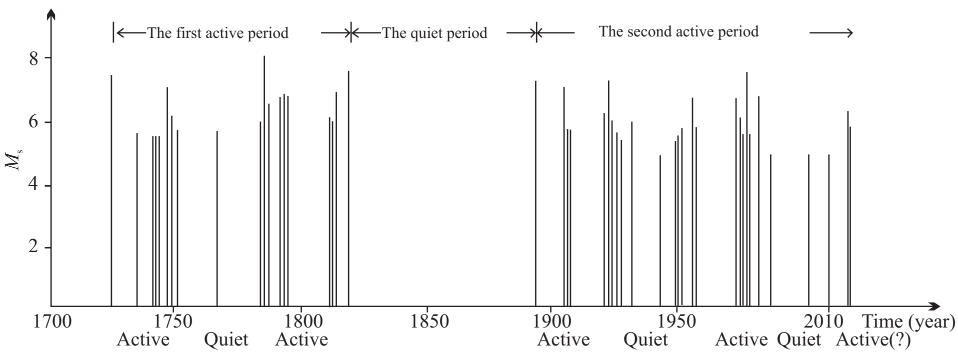

Fig. 8. Time distribution of earthquakes (M_s≥5.0) along the Xianshuihe active fault zone.

$7^3/_4$ earthquake in 1786 and the latest one was the Kangding M_s 6.3 earthquake on November 22, 2014. Among the eight $M_s \geq 7.0$ earthquakes, three happened in the southeast part and five happened in the northwest part. And among the 26 M ≥6.0 earthquakes, eight happened in the southeast part and 18 happened in the northwest part. Except the Yalahe fault, along each of the rest member faults there were $M_s \geq 7.0$ earthquakes to occur, especially along the Luhuo fault and the Daofu fault. Studies of pre-historic earthquakes found many ancient remains (Li et al., 1997; Xu et al., 2005). This can also prove that earthquakes along the Xianshuihe fault zone are frequent and strong.

(2) The seismic activities along the Xianshuihe fault zone have a certain periodicity. According to Deng (1989), Sun et al. (1994), Qian et al. (1988), and Zhou et al. (2001), these years since 1700 can be divided into two active periods and one quiet period. The first active period was from 1700 when the Kangding $M_s > 6.0$ earthquake occurred to 1816 when the Luhuo M_s 7.5 earthquake occurred (Fig. 8), lasting 116 years, during which 14 $M_s >$ 6.0 earthquakes occurred. The following was a quiet period, i.e., from 1817 to 1892, lasting 85 years, during which there were no $M_s > 5.0$ earthquakes. The second active period began from 1893 when the Qianning M_s 7¼ earthquake occurred. By analogy with the first active period of 116 years, the second active period should end in 2008. From 1893 to 2008 there were 13 M > 6.0 earthquakes. However, on April 28, 2010, an M_s 4.5 earthquake occurred in Bamei Town of Daofu County and on November 22, 2014, and an M_s 6.3 earthquake occurred in Tagong grassland of Kangding County. They obviously break the sub-quiet period and have some complicated tendency.

(3) The earthquake genetic faults within the Xianshuihe fault zone are often either migratory or repeated (Fig. 9). Every member fault of the fault zone induced earthquakes in different times, although the Yalahe fault did not induce $M_s \geq 6.0$ earthquakes. This means that the earthquake genetic faults migrate from time to time. According to Qian et al. (1988, 1990), a small ridge near Yousi southwest of Luhuo shows 8 m left-lateral offset, of which 2 m offset was produced by the Luhuo M_s 7.9 earthquake. They thought that the other 6 m offset might be produced by some similar historic earthquakes which were not recorded. Besides, a 5 m left-lateral offset ridge near Wanmuka in Daofu County and some offset terraces near Gelu in Luhuo County both show traces of multiple offsets, and so were also interpreted as results of some historic earthquakes induced by the same faults (Wen et al., 1988). These are one aspect of seismic repeatability. The seismic repeatability is also represented in seismic magnitude. This has already been proved by multiple earthquakes alike in magnitude within the Xianshuihe fault zone. On the other hand, Li et al. (1997) inferred from prehistoric earthquake remains that the time interval of the former address reoccurrence of strong earthquakes at the same position was 200–500 years. And Qian et al.

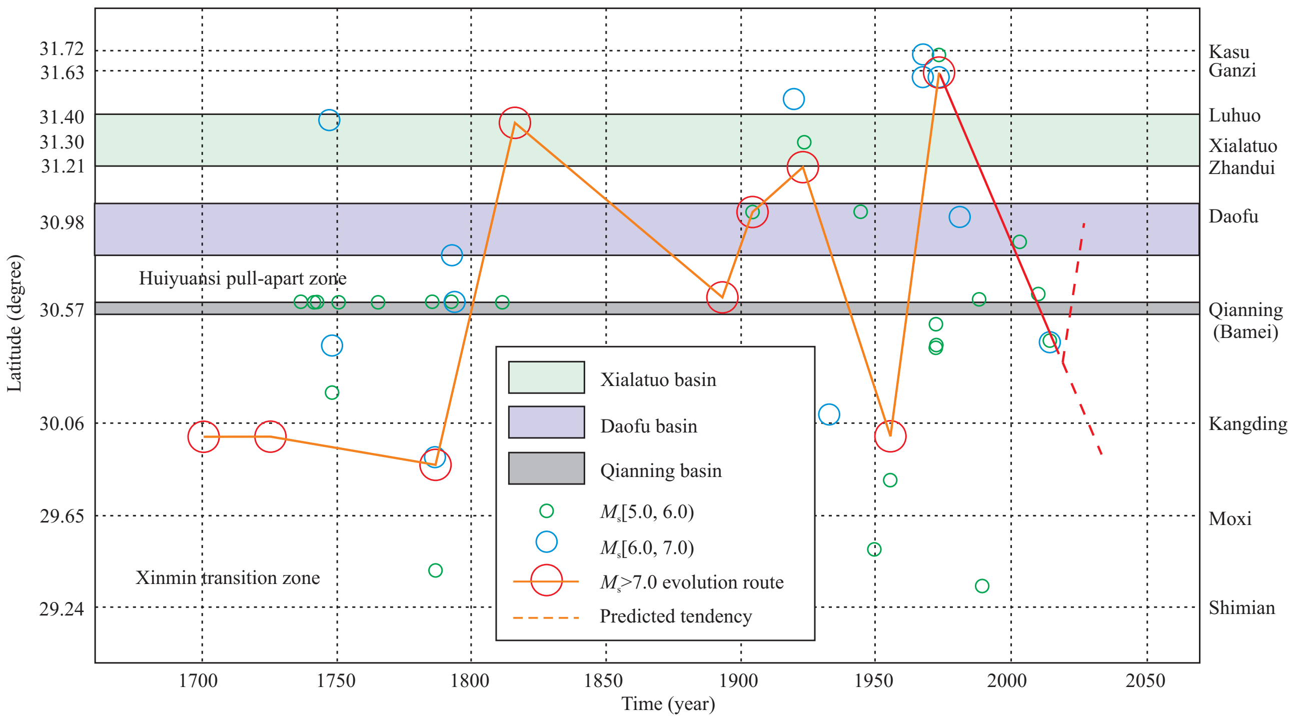

Fig. 9. Space-temporal distribution of $M_s \geq 5$ earthquakes within the Xianshuihe fault zone.

(1990) inferred that the time interval of the former address reoccurrence of another earthquake like the 1973 Luhuo M_s 7.9 earthquake was about 150 years.

5.2 Assessment of strong earthquake risks

The above three characteristics are enough to illustrate the large seismic risk implied by the Xianshuihe fault zone. For such a risk, many researchers have already made their assessments, but different researchers have given different opinions (Qian et al., 1988; Li et al., 1997; Fujii and Matsu'ura, 2000; Zhou et al., 2001; Ran and He, 2006). As an assessment effort, we attempt to approach this problem through the statistical analyses of the frequency of $M_s \geq 5.0$ earthquakes and the quiet time of earthquake genetic faults. i.e., combining the spatial and temporal distribution features of the historical earthquakes, the seismic hazard of the Xianshuihe fault zone has been predicted by using the relationship curve between magnitude and frequency of earthquakes caused by different fault segments.

The known $M_s \geq 5$ earthquakes along the Xianshuihe fault zone and their total number (N) are listed in Table 5, where M_s' are the weighted averages of the magnitudes which were divided in terms of the magnitude interval ΔM_s = 0.5. According to Gutenberg–Richter law (Gutenberg and Richter, 1956), the relationship between the magnitude (M_s) and total number of earthquakes (N) in any given region and time period of at least that magnitude is subject to the following formula:

$$\log N(M_s) = a - bM_s \quad (1)$$

Where M_s is seismic magnitude, N is the total number of $M_s \geq 5.0$ earthquakes, a and b are constants. The related data points are plotted in Fig. 10. Thus we have

$$\log N(M_s) = 9.7068 - 1.1155M_s \quad (2)$$

Where, the obtained fitting correlation coefficient between magnitudes and frequencies is 0.9483.

Considering the previous measured magnitudes are often on the low side, according to the empirical practice, when log $N(M_s)$ = 0 and $M_{smax} = a/b$, b should increase by 0.1–0.5 (Jiang and Dai, 1993). Here, we take 0.1 as a corrected value of b. Thus we have

$$\log N(M_s) = 9.7068 - 1.2155M_s \quad (3)$$

Finally, we obtained that the upper limit magnitude of possible earthquakes within the Xianshuihe fault zone is expressed as: M_u = 9.7068/1.2155 ≈ 8.0 as shown in Fig.10.

As mentioned above, the seismic activities within the Xianshuihe fault zone has the characteristic of reoccurrence along the same fault. Here, we introduced two measures: the average reoccurrence time interval (T_{av}) and the deviation rate (E). The former is an average of the reoccurrence interval of earthquakes along one fault or several faults; the latter (E) is the interval between two real earthquakes / the average reoccurrence time interval (T_{av}). Those two measures are listed in Table 6.

Generally speaking, the relationship between the earthquake reoccurrence risk and the deviation rate (E) is a negative correlation, that is, the smaller the deviation rate is, the higher the earthquake possibility is (Chai et al., 2001; Hori, 2006; Kato et al., 2007; Dieterich, 2009). Table 6 shows that as the possibility of the earthquake reoccurrence risk as are concerned, the deviation rates of each fault segments in the Xianshuihe fault zone are greater than 0.5 at present. Among them, the Qianning fault is the highest, followed by the Daofu fault. Thus it can be predicted that the segment between Daofu and

Table 5 Magnitudes (M_s) and frequencies (N) of $M_s \geq 5$ earthquakes within the Xianshuihe fault zone since 1725

M_s	5.0	5.2	5.5	5.6	5.7	5.8	6.0	6.3	6.5	6.8	6.9	7.0	7.3	7.5	7.6	7.7	7.9
Number	10	1	6	1	1	6	5	1	1	4	1	2	2	2	1	1	1
$N(M_s)$	46	36	35	29	28	27	21	16	15	14	10	9	7	5	3	2	1

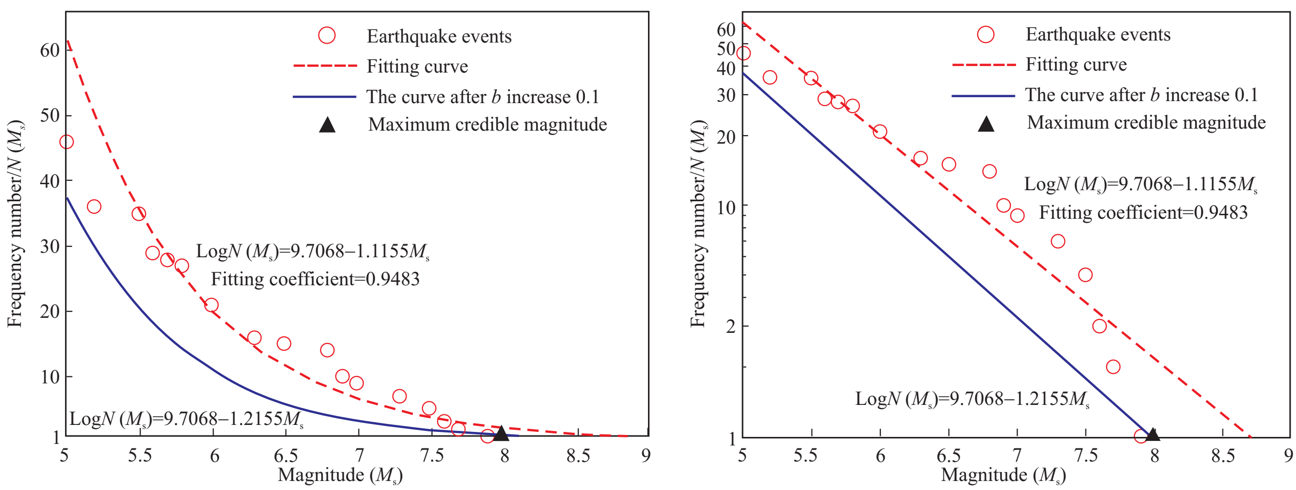

Fig. 10. Magnitude-frequency least squares fitting curves of $M_s \geq 6.5$ earthquake within the Xianshuihe fault zone.

Table 6 Average reoccurrence intervals and deviation rates of $M_s \geq 6.5$ earthquakes within the Xianshuihe fault zone

Fault segment combination	Fault segment	Time	Magnitude (M_s)	Average recurrence interval, Tav (a)	Deviation rate (E)
S1	Luohuo fault	1747	6.8	56.5	0.67
		1811	6.8		
		1816	7.5		
		1967	6.8		
		1973	7.9		
S2	Daofu fault	1923	7.3	38.5	0.78
		1904	7.0		
		1981	6.9		
S3	Qianning fault	1792	6.8	101	1.17
		1893	7.3		
S4	Yalahe fault	-	-	85	0.66
	Zhonggu fault	1748	6.5		
	Zheduotang fault	1955	7.5		
	Kangding fault	1700	7.6		
		1725	7.0		
S5	Moxi fault	1786	7.7	-	-
	Anshunchang fault	-	-		

Qianning (Bamei) would be more likely to occur an earthquake with $M_s \geq 7.0$. Considering the deviation time of the southeast of Xianshuihe fault is long (about 230 years), and despite lack of the recurrence interval data, it also could not be rule out possible earthquakes of about M_s 7.0 occur in the segment from Shimian to Luding.

Comprehensive considering the status of recently occurred seismic geohazards in southwest of China and the advances of geological monitoring technology, it is suggested to establish a GPS or InSAR-based real-time monitoring network of surface displacement to cover the Xianshuihe fault zone as soon as possible (Wang et al., 2009). Such a network can be simultaneously used to monitor the high risk areas of post seismic geohazards by local refinement. And to establish an early warning system of earthquakes and post seismic geohazards to cover the Major residential areas as soon as possible is necessary, too.

6 Conclusions

(1) The Xianshuihe fault zone is an intensely active left-lateral strike-slip fault zone in eastern Tibetan Plateau, which is composed of the Luhuo fault, Daofu fault, Qianning fault, Yalahe fault, Zhonggu fault, Kangding fault, Zheduotang fault and Moxi fault. The Late Quaternary average slip rates of the individual member faults of the Xianshuihe fault zone are different: 10–11.5 mm/a for the Luhuo fault, 10–11 mm/a for the Daofu fault, 8–11 mm/a for the Qianning fault, 8.47±0.92 mm/a for the Moxi fault, 5±1 mm/a for the Zheduotang fault, 7–9 mm/a for the Kangding fault, and 3±1 mm/a for the Zhonggu fault and the Yalahe fault.

(2) The seismic activities within the Xianshuihe fault zone have briefing bright characteristics such as frequent and strong, periodical, and reoccurred. The statistical analyses show that the largest seismic magnitude of possible earthquake within the Xianshuihe fault zone is M_s 8.0. It is predicted that the segment between Daofu and Qianning (Bamei) would be more likely to occur an earthquake with $M_s \geq 7.0$, and it also could not be ruled out that possible earthquakes with about M_s 7.0 occur in the segment from Shimian to Luding.

(3) It is suggested that, both to establish a GPS or InSAR-based real-time monitoring network of surface displacement to cover the Xianshuihe fault zone and to establish an early warning system of earthquakes and post seismic geohazards to cover the major residential areas are very necessary.

Acknowledgments

This research was supported by the Special Project of Basic Work of Science and Technology (grant No. 2011FY110100-2), the Project of China Geological Survey (grant No. 1212010914025 and No. 12120113038000), and the Project of 12th Five-Year National Sci-Tech Support Plan (grant No. 2011BAK12B09).

Manuscript received Aug. 20, 2015
accepted Feb. 19, 2016
edited by Hao Qingqing

References

Allen, C.R., Luo, Z.L., Qian, H., Wen, X.Z., Zhou, H.W., and Huang, W.S., 1991. Field study of a highly active fault zone: The Xianshuihe fault of southwestern China. *Geological Society of America Bulletin*, 103(9): 1178–1199.

Chai Chizhang, Zhang Wenxiao, Liao Yuhua, Xu Wenjun, Shen Xuhui, Tian Qinjian, Wei Kaibo and Chen Zhengwei, 2001. Application of Dangerous Probability Function in Risk Estimation of Surface Rupture Earthquake: Taking Lingwu Faults in Ningxia Region as an example. *Earthquake Research in China*, 17(3): 271–279 (in Chinese).

Chen Guihua, Xu Xiwei, Wen Xueze and Wang Yali, 2008.

Kinematical transformation and slip partitioning of northern to eastern active boundary belt of Sichuan-Yunnan Block. *Seismology and Geology*, 30(1): 58–85 (in Chinese).

Cheng Wanzheng and Yang Yonglin, 2002. Deformation rate changes of tectonic belts along boundaries of Yunnan-Sichuan block and their relation to grouped strong earthquakes. *Crustal Deformation and Earthquake*, 22(4): 21–25 (in Chinese).

Deng Tiangang, 1989. *Xianshuihe Active Fault Zone*. Chengdu: Sichuan Science Press (in Chinese).

Dieterich, J.H., 2009. Applications of rate- and state- dependent friction to models of fault slip and earthquake occurrence. *Earthquake Seismology*, 4, 107–129, Elsevier, B.V., Netherlands.

Fujii, Y., and Matsu'ura, M., 2000, Regional difference in scaling laws for large earthquakes and its tectonic implication. *Pure and Applied Geophysics*, 157: 2283–2302.

Gutenberg, B., and Richter, C.F., 1956. Magnitude and energy of earthquakes. *Annali di Geofisica*, 9: 1–15

He Honglin, Ran Hongliu and Yasutaka IKEDA, 2006. Uniform strike-slip rate along the Xianshuihe-Xiaojiang Fault System and its implications for active tectonics in southeastern Tibet. *Acta Geologica Sinica*, 80(3): 376–386.

He Zexin, Zhang Xujiao, Qiao Yansong, Bao Shuyan, Lu Chunyu and He Xiangli, 2015. Formation of the Yalong downstream terraces in the SE Tibetan Plateau and its implication for the uplift of the Plateau. *Acta Geologica Sinica* (English Edition), 89(2): 542–560.

Heim, A., 1934. Earthquake region of Taofu, Chinese Tibet. *Geological Society of America Bulletin*, 45: 1035-1049.

Hori, T., 2006, Mechanisms of separation of rupture area and variation in time interval and size of great earthquakes along the Nankai Trough, southwest Japan. *Journal of the Earth Simulator*, 5: 8–19.

Jiang Pu and Dai Lisi, 1993. *Conspectus of engineering seismology*. Beijing: seismological press (in Chinese)

Kato, N., Lei, X., and Wen, X., 2007. A synthetic seismicity model for the Xianshuihe fault, southwestern China: Simulation using a rate- and state-dependent friction law. *Geophysical Journal International*, 169 (1): 286–300.

Li Hailong, Zhang Yueqiao, Zhang Changhou, Dong Shuwen and Zhu Fusheng, 2015. Middle Jurassic syn-kinematic magmatism, anatexis and metamorphism in the Zheduo-Gonggar massif, implication for the deformation of the Xianshuihe fault zone, East Tibet. *Journal of Asian Earth Sciences*, 107: 35–52.

Li Tianshao, Du Qifang and You Zeli, 1997. *The Active Xianshuihe Fault Zone and Seismic Risk Assessment*. Chengdu: Cartographic Publishing House of Chengdu (in Chinese).

Li Xi, Ran Yongkang, Chen Lichun, Wu Fuyao, Ma Xinquan and Cao Jun, 2015. Late Quaternary large earthquakes on the western branch of the Xiaojiang Fault and their tectonic implications. *Acta Geologica Sinica* (English Edition), 89(5): 1516–1530.

Lu Yipei and Liao Hua, 2001. Dynamic evolution characteristic of deformation, gravity and geo-magnetism fields. *Earthquake Research in Sichuan*, (3):11–16 (in Chinese).

Meade, B.J., 2007. Present-day kinematics at the India-Asia collision zone, *Geology*, 35(1): 81–84.

Molnar, P., and Dayem, K.E., 2010. Major intracontinental strike-slip faults and contrasts in lithospheric strength. *Geosphere*, 6(4): 444–467.

Peng Jinchuan, Liao Hua, Gu Tie and Zhang Yi, 2007. Motion characteristics of the Xianshuihe fault based on observation data of GPS continuing-run reference stations. *Earthquake Research in Sichuan*, (4):14–17 (in Chinese).

Qian Hong, Allen, C.R., Luo Zhuoli, Wen Xueze, Zhou Huawei and Huang Weishi, 1988. The active characteristics of Xianshuihe Fault in Holocene. *Earthquake Research in China*, 4(2): 9–18 (in Chinese).

Qian Hong, Luo Zhuoli and Wen Xueze,1990. Preliminary study of characteristic earthquakes in the Xianshuihe Fault zone. *Acta Seismologica Sinica*, 12(1): 22–29.

Qiao Xuejun, Wang Qi and Du Ruilin, 2004. Characteristics of current crustal deformation of active blocks in the Sichuan-Yunnan region. *Chinese Journal of Geophysics*, 47(5): 805–811 (in Chinese).

Ran Hongliu and He Honglin, 2006. Research on the magnitude and recurrence interval of characterized earthquakes with Magnitude≥6.7 along the northwestern portion of the Xianshuihe fault zone in western Sichuan, China. *Chinese Journal of Geophysics*, 49 (1):153–161 (in Chinese).

Roger, F., Calassou, S., Lancelot, J., Malavieille, J., Mattauer, M., Xu, Z.Q., Hao, Z.W., and Hou, L.W., 1995. Miocene emplacement and deformation of the Konga Shan granite (Xianshui He fault zone, west Sichuan China): Geodynamic implications. *Earth and Planetary Science Letters*, 130(1-4): 201–216.

Sun Jianzhong, Shi Shunying, Zhou Shuoyu and Zhang Aihua, 1994. Inversion of the present kinematic characteristics of Xianshuihe fault zone from seismic moment tensor. *Crustal deformation and earthquake*, 14(4): 9–14 (in Chinese).

Schwartz, D.P., and Coppersmith, K.J., 1984. Fault behavior and characteristic earthquakes: example from the Wasatch and San Andreas fault zones. *Journal of Geophysical Research*, 89 (B7): 5681–5698.

Tang Rongchang and Han Weibin, 1993. *Active Faults and Earthquakes in Sichuan Province*. Beijing: Seismological Press (in Chinese).

Tang Rongchang, Qian Hong, Zhang Wenfu, Zhang Chenggui, Cao Yangguo and Liu Shengli, 1984. On the seismogeological setting and conditions of seismogenic structure of 1981 Daofu earthquake. *Seismogeology*, 6(2): 28–37 (in Chinese).

Tang Rongchang, Wen Dehua, Deng Tiangang and Huang Shengmu, 1976. A Preliminary study on the characteristics of the ground fractures during the Luhuo M =7.9 earthquake, 1973 and the origin of the earthquake. *Chinese Journal of Geophysics*, 19(1): 28–27 (in Chinese).

Tang Wenqing, Chen Zhiliang, Liu Yuping, Zhang Qingzhi, Zhao Jixiang, Burchfiel, B.C., and King, R.W., 2005. Present-day tectonics activity in the intersection area of the Xianshuihe fault and Longmenshan Fault on the eastern margin of the Qinghai-Tibet plateau. *Geological Bulletin of China*, 24(12): 1169–1172 (in Chinese).

Tang Wenqing, Zhang Qingzhi, Pan Zhongxi, Li Jun and Yang Cheng, 2015. Crustal motion characteristics in the eastern margin of the Tibetan Plateau and adjacent regions after the Wenchuan earthquake. *Acta Geologica Sinica* (English Edition), 89(5): 1690–1701.

Tapponnier, P., Xu, Z., Roger, F., Meyer, B., Arnaud, N., Wittlinger, G., and Yang, J.S., 2001. Oblique stepwise rise and growth of the Tibet Plateau. *Science*, 294: 1671–1677.

Wang, E., Meng, K., Su, Z., Meng, Q., Chu, J. J., Chen, Z., Wang, G., Shi, X., and Liang, X., 2014. Block rotation: Tectonic response of the Sichuan basin to the southeastward growth of the Tibetan Plateau along the Xianshuihe-Xiaojiang fault, *Tectonics*, 33, 1–32.

Wang, H., Wright, T.J., and Biggs, J., 2009. Interseismic slip rate of the northwestern Xianshuihe fault from InSAR data. *Geophysical Research Letters*, 36 (3): L03302.

Wang Min, Shen Zhengkang, GanWeijun, Liao Hua, Li Tieming, Ren Jinwei, Qiao Xuejun, Wang Qingliang, Yang Yonglin, and Li Peng, 2008. GPS monitoring of temporal deformation of the Xianshuihe Fault. *Science in China* (Ser D), 38(5): 575–581 (in Chinese).

Wang, Q., Zhang, P.Z., Freymuller, J.T., Bilham, R., Larson, K.M., Lai, X., You, X., Niu, Z., Wu, J., Li, Y., Liu, J., Yang, Z., and Chen, Q., 2001. Present-day crustal deformation in China constrained by Global Positioning System measurements. *Science*, 294(5542): 574–577.

Wang, S., Fang, X., Zheng, D., and Wang, E., 2009. Initiation of slip along the Xianshuihe fault zone, eastern Tibet, constrained by K/Ar and fission-track ages. *International Geology Review*, 51(12): 1121–1131.

Wen Xueze, Allen, C.R., Luo Zhuoli, Qian Hong, Zhou Huawei and Huang Weishi, 1989. Segmentation, geometric features, and their seismotectonic implications for the Holocene Xianshuihe Fault zone. *Acta Seismologica Sinica*, 11(4):362–371.

Wen Xueze, Jia Jinkang and Pan Mao, 1988. Recent slip rates, earthquake recurrence intervals and strong seismic hazards on the northwestern segment of the Xianshuihe fault zone. *Earthquake Research in China*, 2(4): 432–451.

Xiong Tanyu, Yao Xin and Zhang Yongshuang, 2010. A review on study of activity of Xianshuihe fault zone since the Holocene. *Journal of Geomechanics*, 16(2): 102–113 (in Chinese).

Xu, G.Q., and Kamp, P.J.J., 2000. Tectonics and denudation adjacent to the Xianshuihe Fault, eastern Tibetan Plateau: Constraints from fission track thermochronology. *Journal of Geophysical Research*, 105(B8): 231–251.

Xu Xiwei, Cheng Guoliang, Yu Guihua, Song Fangmin, Xiang Hongfa, Zhang Lanfeng, Ron Hagai, Wang Yanglong and Wen Xueze, 2003. Tectonic and paleomagnetic evidence for the clockwise rotation of the Sichuan-Yunnan rhombic block. *Seismology and Geology*, 25(1): 61–70 (in Chinese).

Xu Xiwei, Zhang Peizhen, Wen Xueze, Qin Zunli, Chen Guihua and Zhu Ailan, 2005. Features of active tectonics and recurrence behaviors of strong earthquakes in the western Sichuan Province and its adjacent regions. *Seismology and Geology*, 27(3): 446–461 (in Chinese).

Xu, Z.Q., Hou, L.W., Wang, Z.X., Fu, X.F., and Huang, M.H., 1993. *Orogenic Processes of the Songpan-Ganze Orogenic Belt of China*. Beijing: Geological Publishing House.

Yan Bing and Lin Aiming, 2015. Systematic deflection and offset of the Yangtze River drainage system along the strike-slip Ganzi-Yushu-Xianshuihe Fault Zone, Tibetan Plateau. *Journal of Geodynamics*, 87: 13–25.

Yang Yonglin and Su Qin, 2007. Study on present activity characteristics of Xianshuihe fault zone. *Journal of Geodesy and Geodynamics*, 27(6): 22–27 (in Chinese).

Zhang, P.Z., Peter, M., and Xu, X.W., 2007. Late Quaternary and present-day rates of slip along the Altyn Tagh fault, northern margin of the Tibetan Plateau. *Tectonics*, 26: TC5010, doi: 10.1029/2006TC002014.

Zhang, Q., Zhang, P., Wang, C., Wang, Y., and Ellis, M.A., 2003. Earthquake triggering and delaying caused by fault interaction on Xianshuihe fault belt, southwestern China. *Acta Seismologica Sinica*, 16(2): 156–165.

Zhang Yongshuang, Yao Xin, Xiong Tanyu, Ma Yinsheng, Hu Daogong, Yang Nong and Guo Changbao, 2010. Rapid identification and emergency investigation of surface ruptures and geohazards induced by the M_s 7.1 Yushu earthquake. *Acta Geologica Sinica* (English edition), 84 (6): 1315–1327.

Zhang Yongshuang, Yao Xin, Hu Daogong, Guo Changbao and Xiong Tanyu, 2012. Quantitative zoning assessment of crustal stability along the Yunnan–Tibet railway line, Western China. *Acta Geologica Sinica* (English Edition), 86(4):1004–1012.

Zhang Yueqiao, Chen Wen and Yang Nong, 2004. 40Ar/39Ar dating of shear deformation of the Xianshuihe fault zone in west Sichuan and its tectonic significance. *Science in China* (Ser D), 34(7): 613–621 (in Chinese).

Zhang, Y.Q., Dong, S.W., Hou, C.T., Shi, J.S., Wu, Z.H., Li, H.L., Sun, P., Liu, G., and Li, J., 2013, Seismogenic structure of the April 20, 2013, Lushan M_s 7 earthquake in Sichuan, *Acta Geologica Sinica* (English edition), 87(3): 633–645.

Zhou Rongjun, He Yulin, Huang Zuzhi, Li Xiaogang and Yang Tao, 2001. The slip rate and strong earthquake recurrence interval on the Qianning-Kangding segment of the Xianshuihe fault zone. *Acta Seismologica Sinica*, 14(3): 263–273.

About the first author

ZHANG Yongshuang, Male; born in 1968 in Yantai City, Shandong Province; doctor degree; research professor of Institute of Geomechanics, Chinese Academy of Geological Sciences; He is now interested in the study on active faults and engineering geology and geohazards.

E-mail: zhys100@sohu.com; phone: 010-88815560.